International Journal of ChemTech Research
CODEN (USA): IJCRGG, ISSN: 0974-4290, ISSN(Online):2455-9555
Vol.9, No.09 pp 588-597, 2016

Synthesis of Mesoporous Carbon using Gelatin as A Carbon Source and SBA-15 as A Template for Dibenzotiophene Adsorption

Maria Ulfa, Wega Trisunaryanti*, Iiplzul Falah, Sutarno,Indriana Kartini

Department of Chemistry, Facultyof mathematicsandnatural sciences UniversitasGadjahMada, Sekip Utara, Yogyakarta, Indonesia 55281

Abstract : Synthesis of mesoporous carbon using bovine bone gelatin as the carbon precursor and SBA-15 as a template for dibenzothiophene adsorption had been investigated. The Gelatin was infiltrated onto the SBA-15 template by carbonization step at 110 and 160 °C for 7 h followed by pyrolysis at 900 °Cfor 3 h under argon atmosphere. The carbon had a specific surface area of 760 m^2/g, total pore volume of 0.999 cm^3/g, average pore diameter of 5.2 nm, a meso-poresquantity of 74 % and a narrow pore size distribution that was dominant at 4.5 nm. Dibenzotiophene (DBT) was used as a model of fuels fraction for adsorption study using the mesoporous carbon as an adsorbent.This paper investigated the equilibrium, kinetics and thermodynamics of the adsorption of the DBT. Kinetic studies were investigated by Lagergren, HoMcKay and Pandey equation. The equilibrium obtained within 70 min. It was found that the adsorption kinetic followed a pseudo-second-order rate equations. While, the adsorption equilibrium followed the Langmuir isotherm model, with the maximum adsorption capacity of 66.6 mg/g-carbon.
Keywords: mesoporous carbon, gelatin, dibenzotiophene, adsorption.

Introduction

Mesoporous carbon is an interesting material for many applications such as adsorbents, catalysts, catalysts supports and electrodes materials due to its high periodicity of framework and large surface area and narrow pore size distribution[1-3]. The mesoporous carbon was synthesized from different organic compounds as carbon precursors including sucrose, furfuryl alcohol, surfactants, and polymer[4-7].One of the potential polymer as source of carbon is gelatin due to high carbon content, a lot of amine as the functional group which have high affinity interaction to silica species[8] template, abundant and biodegradable. Mesoporous carbon were successfully synthesized by using gelatin as carbon precursor[8-13]. However, the application of the mesoporous carbon obtained in the previous work is still limited.

The high porosities character of mesoporous carbon has a lot of benefit for the clean hydrocarbon fuels production. One of tremendous challenge in the modern petroleum refinery is particularly of the high sulfur content in the fuels. This could potentially lead to acid rain and degradation of the converters in cars. In order to overcome this problem, sulfur was removed through desulfurization[14,15] or adsorption process from the fuel. Adsorption treatment is regarded to be an attractive approach, due to the low energy consumption and high sulfur removal efficiency[16-22].

Several adsorption models have been investigated. Most of these have been reported to follow a first

order kinetic process. The irreversible of pseudo-first order rate equation of Lagergren has long been widely applied[23]. The correlative kinetic analysis of Ho and McKayto the irreversible sorption process has been reported from the experimental data by the pseudo-second order rate[24]. The kinetic analysis of Pandey as the reversible sorption process obtained by the pseudo-first order rate[23].However, the studies on the determination of the best DBT adsorption system by different equation of order rate based on the fundamental assumption is still not well studied.

In the present work the new carbonaceous materials were synthesized by carbonization and pyrolysis of bovine bone gelatin deposited on the SBA-15. The morphology and structure were studied by TEM and SAXRD, respectively. Meanwhile, pore characteristics of the carbon material were evaluated by using N_2 adsorption-isotherm analysis. The carbon has been studied for sulfur removal application using dibenzotiophene solution as a fuel model. The kinetic experimental data was evaluated using Lagergren, Ho and McKay and Pandey Model. Meanwhile, the equilibrium and thermodynamic of the adsorption process were studied by Langmuir isotherm.

Experimental

Chemical

All the chemicals used in this work were analytical reagent grade purchased from Sigma-Aldrich Co. Dibenzotiophene was procured from Merck, Germany. The n-Hexane was obtained from Aldrich Chemicals. Gelatin was extracted from Javanese cow bone by acid treatment, as has been described elsewhere[12]. The SBA-15 as the silica template was supplied by Green Stone, Swiss (particle size: 0,1μm, pore diameter: 8-9 nm, surface area: 550 m^2/g, and pore volume: 1,0 cm^3/g).

Sample preparation

The synthesis of mesoporous carbon were conducted by sequential impregnation using one gram of a template (SBA-15) which added to a solution obtained by dissolving 1 g of gelatin into a solution (water:H_2SO_4 = 50:0.2 v/w) at temperature 60 °C and keeping the mixture in an oven for 7 h at 110 °C. Subsequently, the oven temperature was raised to 150 °C for 7 h. In order to obtain fully carbonized gelatin inside the pores of the silica template, gelatin solution was added to the pre-treated sample and the mixture was subjected to the thermal treatment described above. The template–polymer composites were then pyrolyzed in a nitrogen flow at 900 °C and kept under these conditions for 3 h to carbonize the polymer. The mesoporous carbon was recovered after dissolution of the silica framework in HF 10%for 24 h by stirring process. The obtained carbon was cleaned by filtration, washed several times with ethanol, and dried at 120 °C produced the mesoporous carbon from gelatin denoted as MCG.

Characterization

Nitrogen adsorption and desorption isotherms were measured on a Quantachrome Autosorb 1 sorption analyzer. All samples were outgassed at 300 °C for 3 h prior to the nitrogen adsorption measurements. The specific surface area was calculated using the Brunauer–Emmett–Teller (BET) method. The pore size distributions were obtained from the adsorption branch of the nitrogen isotherms by Barrett–Joyner–Halenda (BJH) method. The morphologies of all the synthesized samples were characterized by a transmission electron microscopy (TEM) instrument (Philips CM30) operating at 120 kV. Each sample was dispersed in absolute ethanol and a drop was placed on a Cu grid covered with perforated carbon film. Small-angle powder X-ray diffraction (SAXRD) pattern was recorded with a Bruker D4 powder X-ray diffractometer (Germany) using Cu Kα radiation (40 kV, 40 mA) conducted for analyzing the ordering of the MCGmeso-structure.

Adsorption

Stock solution of sulfur having 1 g/l concentration was made by dissolving 100 mg of DBT in 200 mL of n-hexane. The range of concentration of sulfur solutions prepared from the stock solution by diluting with n-hexane varied between 10 and 500 mg/l. The procedure for adsorption of the DBT onto the MCG included addition of 50 mg of the adsorbent into 10 mL of the stock solution and stirring at room temperature for 60 min. The adsorbent was separated from the solution by a Whatman filter paper and the solution was subjected to UV–Vis instrumentation. The measurements were performed in the range of 200–400 nm. The equilibrium

concentration of DBT at different stages was measured from the calibration curve obtained at k_{max} of 326 nm (R^2 = 0.999). The amount of DBT adsorbed (q_e) by the adsorbent was calculated using the following equation:

$$q_e = (C_o - C_e)x\frac{w}{m} \quad (1)$$

where and are the initial and equilibrium concentrations of DBT in the bulk phase, respectively, w is the amount of the liquid phase (L) and m is the amount of adsorbent (g). The amounts of DBT adsorbed onto the adsorbents at any time (q_t) were obtained from equation:

$$q_t = (C_o - C_t)x\frac{w}{m} \quad (2)$$

Where q_t is the bulk concentration of DBT at any time t.

Result and Discussion

Nitrogen adsorption–desorption isotherms and their corresponding pore size distribution curves of the MCG carbons sample prepared using gelatin by sequential impregnation were shown in Fig. 1.The obtained isotherm of the MCG carbon sample can be classified as type IV in according to the IUPAC classification and exhibited a H2 type hysteresis loop indicating that it is a mesoporous material with tubular pores[13]. The narrow pore size distribution of MCG sample was dominant at about 4.5 nm. A similar result was obtained from TEM investigations. The average pore diameter of the MCG carbon sample calculated using the BJH method is approximately 5.2 nm which is obtained from desorption branch. The specific surface area of the MCG mesoporous carbon materials was 760 m^2/g. The P/Po position of the inflection point is a function of the pore diameter due to the completion of the adsorption procedure on the surface and the formation of mono or multilayer[23-27]. The inflection of the MCG isotherm in P/Po range from 0.0 to 1.0 which is divided into three region. At the first inflection point (entry pressure, P/Po< 0.05), nitrogen occupies only a small fraction of the pore volume containing the smaller pores represent the monolayer formation of microporous carbon. Next, much of the larger pore space becomes filled with nitrogen with a comparatively slight increase in pressure (P/Po 0.4-0.8) which is reflected the contribution of mesopores carbon to the adsorption. These sharp inflection of the mesoporous carbon MCG isotherm, at which the nitrogen uptake suddenly occurs, might be due to the capillary condensation of nitrogen inside the mesopores which is characteristic for uniform pores. After capillary condensation step, a long plateau at higher relative pressures is associated with the multilayer adsorption of nitrogen at the external surface and interstitial voids of MCG sample. The shallow slope of this region indicates that the external surface area of the MCG sample is so small. The desorption branch almost coincides with adsorption branch which reveals the reversible nitrogen adsorption inside the mesopores. Finally, large pressure increases (P/Po >0.8) are required to force more nitrogen into the macroporous carbon.

The specific surface area of the MCG mesoporous carbon materials (760 m^2/g) was higher than that of the SBA-15 template (550 m^2/g) as showed in Table 1. The higher surface area of the MCG could be attributed by the surface heterogeneity and micropores in the materials because of the contribution from the microporosity within the carbon walls. It is also contributed by the extra porosity due to the incomplete replication process. It can be concluded that the SBA-15 sample contain micropores lower than the MCG that confirmed by calculating result of mesoporous percentage (Table 1) and isotherm adsorption result. It can be explained by adsorption phenomena. In the MCG sample, micropores assumed to be slit-like in carbons, adsorbed molecules interact with two surfaces, as opposed to just one on an open surface. As on the MCG, at low pressure the monolayer is formed clearly indicating the presence of micropores. The situation is different for theSBA-15, whereas adsorption at low P/Po is very small and the general shape of the isotherm resembles to a certain degree. The MCG sample showed narrow pore size distribution dominant at 4.5 nm, but the SBA-15 showed a relatively broader pore-size distribution centered at 8.6 nm indicating the successful of silica dissolution. The pore volume of the MCG (0.99 cm^3/g) materials is close to the SBA template (1.02 cm^3/g) due to presence of microporous as explained above[25]. All the trend of nitrogen adsorption desorption result was similar to the previous reports of others mesoporous carbon materials[25-35].

Table 1. Textural Parameter of SBA-15 and mesoporous carbon (MCG) sample

Sample	S_{BET} (m^2/g)	S_{me} (m^2/g)	% me	Vt (cm^3/g)	D^{BJH} (nm)	D^{TEM} (nm)	a_o (nm)	t= a_o- D^{TEM} (nm)
SBA-15	556	515	95	1.02	8. 76	8.58	11.58	2.82
OMCG	756	559	74	0.999	5.20	4.47	10.39	5.92

Vt= total pore volume; D= diameter, t=wall thickness

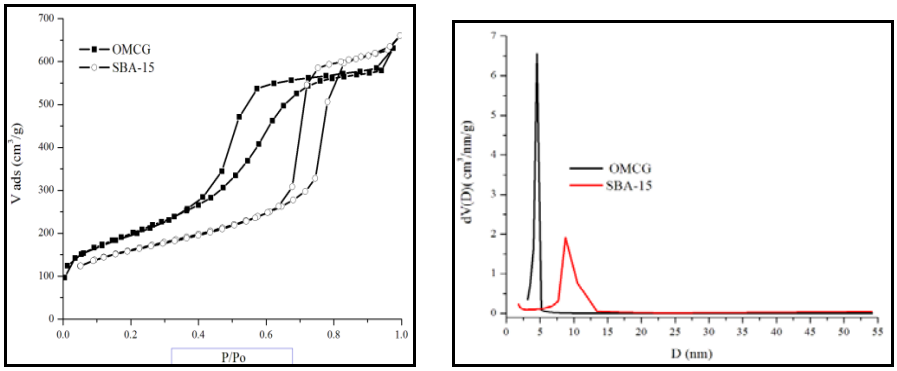

(a) (b)

Fig. 1. a) Nitrogen adsorption–desorption isotherms and b) pore size distribution of the samples

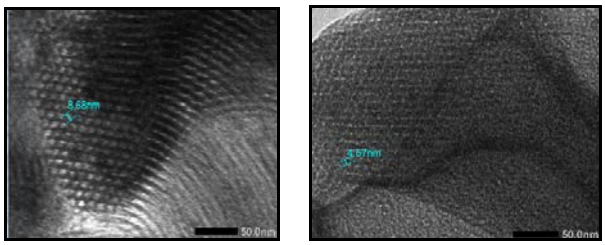

(a) (b)

Fig. 2. Top view TEM images of a) SBA-15 and b) MCG sample.

The morphologies of the synthesized mesoporous carbon MCG samples and SBA-15 were characterized by TEM in Fig.2. Top view TEM images showed the uniform pore size of MCG and SBA-15 to be about 4.5 and 8.5 nm, respectively. This results confirm the pore size distribution obtained by nitrogen adsorption desorption. The mesoporous carbon MCG shows the same well ordered hexagonal structure (space group p6*mm)* as previously report[25-29]The resultant carbon particles have exactly the same morphology as that of the SBA-15 silica particles. On the other hand, although the mesoporous carbon MCG have exactly the same morphology as that of the SBA-15 silica, the presence of stacking faults can be found in TEM indicating the pore structure of carbon disordered which as explained by other researchers[31-34].

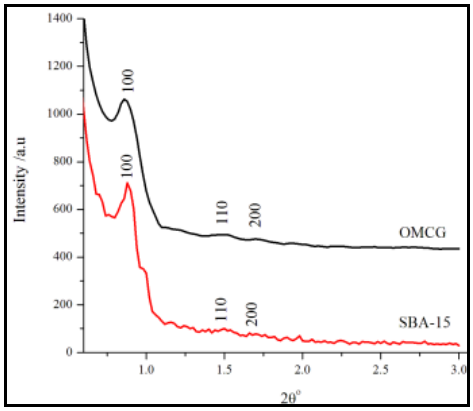

Fig. 3. Small-angle XRD (SAXRD) patterns of SBA-15 and OMCG

The SAXRD pattern (Fig. 3) of the observed carbonaceous material OMCG show three well resolved peaks (at 2θ around 0.8°; 1.6° and 1.8°) indexed as (1 0 0), (1 1 0) and (2 0 0), characteristic of the two-dimensional hexagonal space group p6*mm* indicating that OMCG have retained the ordered structure of their parent silica template as previously report[29-32]. The (100) peaks of OMCG are lower than SBA-15. It is indicating the result of structural shrinkage during replication process[35]. Intensities of these characteristic peaks indicate that OMCG is probably finely disordered in the small part of samples which is confirmed by the result of nitrogen adsorption-desorption and TEM.

As can be seen in Table.1 and Fig. 3, the diffraction peaks of the mesoporous carbons OMCG and SBA-15 are clearly observed which can be related to some d-spacings values. The lattice parameter (a_o) of SBA-15 was determined to be 10.6 nm, its wall thickness is calculated to be approximately 2.82 nm, which is close to the half of average pore diameter of OMCG (5.2 nm) calculated by BJH of nitrogen adsorption. Interestingly, the percentage difference of lattice parameter between SBA-15 to OMCG (10%) is close to the difference of average pore diameter OMCG (8%) calculated by wall thickness and BJH nitrogen adsorption data.It is can be explained by replication process.

The pore formation of mesoporous carbon sample generated by replication process of SBA-15 were explained in the previous[21-25]. The SBA-15 has pore structure with a hexagonal arrangement of straight pores, there are also some micropores like in zeolite pore[34] or small mesopores in the wall, connecting the main channels as bridges. When the carbon precursor fills the whole inner space, the framework of nanorod carbon can be produced. Since the silica framework has been removed, the space of the silica wall now becomes empty channels of carbon, which mean the pore size of carbon was twice of that SBA-15 wall thickness size at a nanometer scale. Although OMCG has a similar pore structure to that of SBA-15, some stacking faults on the OMCG carbon sample were observed by TEM, SAXRD and isotherm adsorption. The stacking faults due to some shrinkage that inevitably occurs during the carbonization process and subsequent dissolution of the silica framework, a smaller pore diameter is expected for the carbon replica[33]. If the pore system within the OMCG carbon sample is perfectly replicated, we expect the basic structure in the final products is a three dimensional arrangement of solid nanopipe with mesoporous size connected with each other by some very short nanorod as the report previolusly[28-33].

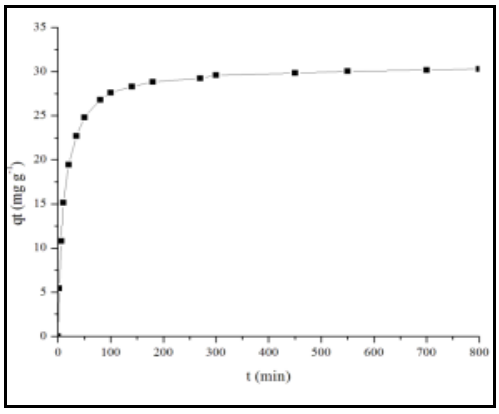

Fig. 4. Effect of the contact time on DBT adsorption capacity onto MCG at 30 °C.

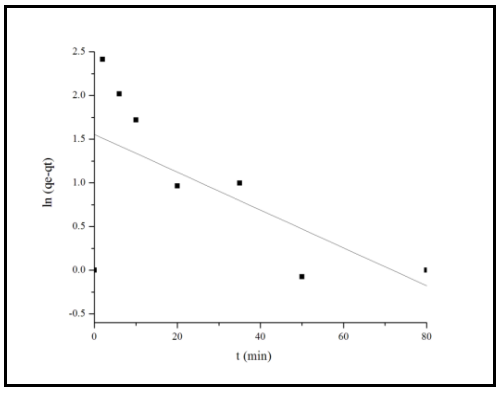

Fig. 5. Pseudo-first-order linear by Lagergren plots for the removal of DBT by MCG

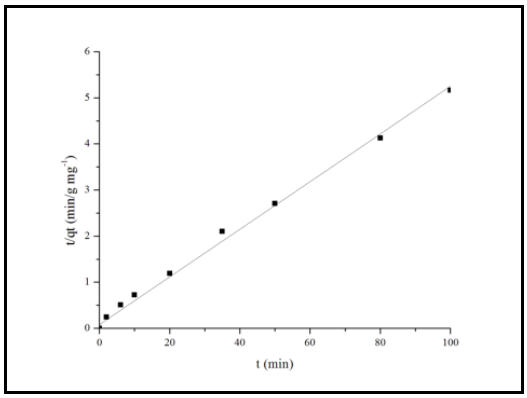

Fig. 6. Pseudo-second-order linear by Ho and McKay plots for the removal of DBT by MCG

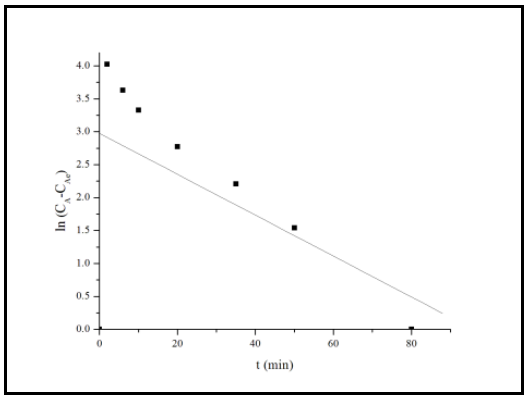

Fig. 7. Pseudo-first-order linear by Pandey plots for the removal of DBT by MCG

Fig. 4 presents a representative plot of the time-course of DBT onto MCG. The adsorption of DBT is found to be very rapid during the first 50 min. but gradually decreased and finally reached equilibrium after 5h of contact time. This indicates that a large number of vacant surface sites are available for adsorption during the initial stage, and after certain time, the remaining vacant surface sites are difficult to be occupied due to repulsive forces between the solute molecules on the solid and bulk phases The adsorption equilibrium model used in this study is the Langmuir equation which was derived from the sorption rate equation[24]. The sorbate DBT occupies n sites and the rate equation is obtained by combining the forward adsorption rate step and the reverse desorption step. When the sorption reaction reaches equilibrium, the Langmuir equation results:

$$\frac{C_e}{q_e} = \frac{C_e}{q_m} + \frac{1}{Kq_m} \quad (3)$$

The Langmuir constant (K_L) can be used to calculate the Gibbs free energy change (ΔG^o) according to the following equation.

$$\mathbf{-RT\ Ln\ K_L = \Delta G^o}$$

The value of ΔG^o was calculated to be−15.4 kJ mol^{-1}, indicating that the DBT adsorption by MCG adsorbent was a endothermic physisorption process, that is similar to the result of k sorption derived from pseudo second order model. The adsorption process from whole experiment predicted that the system of DBT-mesoporous carbon and hexane consist of two process which is the species of DBT adsorbed onto MCG and the hexane molecules desorbed out of MCG due to the displacing hexane molecule by DBT.

The design of industrial DBT adsorption can be predicted by using the system of kinetics DBT adsorption. The kinetic of DBT equations are required in the design of an adsorption system and their subsequent optimization. Therefore it is important to establish the most appropriate correlation for the kinetic isotherm curves. This paper tried to use the three kinetic equations namely irreversible pseudo first order, irreversible pseudo second orderand reversible pseudo first order obtained by Lagergren, Ho And McKay and

Pandey, respectively. For each kinetic system and equation, all the experimental data were used. The percent standard deviation error function was employed in this study to find out the most suitable kinetic model to represent the experimental data.

The kinetic data of DBT irreversible adsorption have been tested by the pseudo first-order of Lagergren models using the following equations:

$$\frac{dq_t}{dt} = k_1(q_e - q_t) \quad (4)$$

$$\frac{dq_t}{(q_e - q_t)} = k_1 dt \quad (5)$$

$$ln(qe - qt) = \ln qe - k_1 t \quad (6)$$

Fig. 5 showed the result of the calculated parameters obtained by plotting ln(qe–qt) versus t for the pseudo-first-order model with the corresponding correlation coefficients (R^2) values are 0.760.

The irreversible DBT adsorption of kinetic data have been evaluated by the pseudo-second-order of Ho and McKay models using the following equations:

$$\frac{dq_t}{dt} = k_1(q_e - q_t)^2 \quad (7)$$

$$\frac{dq_t}{(q_e - q_t)^2} = k_1 dt \quad (8)$$

On integration the Ho and McKay rate equation with boundary condition $q = qt$ at $t = t$ and $q = 0$ at $t = 0$ becomes:

$$-\int_0^{q_t} \frac{1}{(q_e - q_t)^2} d(q_e - q_t) = \int_0^t k_1 \quad dt \quad (9)$$

$$q_t = \frac{{q_e}^2 k_1 t}{q_e k_1 t + 1} \quad (10)$$

The modified of Eq 10 becomes:

$$\frac{t}{q_t} = \frac{t}{q_e} + \frac{1}{{q_e}^2 k_1} \quad (11)$$

The calculated parameters obtained by plotting *t/qt*versus *t* for the pseudo-second-order model with the corresponding correlation coefficients (R^2) values are 0.999 shown at Fig. 6.

The reversible system of pseudo-first order equation by Pandey model was used to correlate into the experimental data based on the mechanistic scheme shown in Eq 12.A molecule of DBT was assumed to sorb on one sorption site of mesoporous carbon surface.

$$A_{(solid)} + S_{(DBTsolution)} \rightleftharpoons A \quad (12) \quad \text{(Adsorbed phase)}$$

where A is a sorption site on the solid. The reversible DBT adsorption of kinetic data have been evaluated by the pseudo-first-order of Pandey models using the following equations:

$$\frac{-dC_A}{dt} = k_{ads} C_A - k_{des} C_{AS} \quad (13)$$

$$\ln(C_A - C_{Ae}) = -(k_{ads} - k_{des})t + \ln(C_{Ao} - C_{Ae}) \quad (14)$$

where$k_{ads}$and k_{des} (g mg^{-1} min^{-1}) are the adsorption and desorption rate constants. The calculated parameters obtained by plotting ln *C*versus *t* for the pseudo-first-order model with the corresponding correlation coefficients (R^2) values are 0.992 shown at Fig. 7.

Table 2. Kinetic model for adsorption of DBT on OMCGmesoporous carbons

Assumption	order	Model	qm	ks	kd	K=ks/kd	R^2
Irreversible	Pseudo First	Lagergren	qe=10.7	0.023			0.784
Irreversible	Pseudo Second	Ho and McKay	qe=44.8	0.029			0.999
Reversible	Pseudo First	Pandey		0.213	0.23	0.049	0.992

The best-fit values of k_{ads}, $k_{des}$and k (k_{ads}/ k_{des}), qe, qmax with coefficient correlation for the pseudo first order, pseudo second order models and from Langmuir for DBT adsorption onto mesoporous carbon OMCGgiven in Table 2. The results indicate that there is no linear correlation between ln(qe–qt) and t (R^2= 0.760) (Fig. 6), so that the kinetic of DBT adsorption onto OMCG cannot be described by the pseudo-first-order model. However, the data are very well fitted to the pseudo-second-order model (Fig. 7) and the correlation coefficient is close to unity (R^2=0.999), indicating that the DBT adsorption onto OMCG can be described by this Ho and McKay kinetic model. Furthermore, Fig. 7 showed that the plot of *t/qt* versus *t* is linear over the whole time range, suggesting that the adsorption is at least a two step process with the first step being the film diffusion. The second step can be attributed to pore diffusion. The overall kinetic survey suggests that the pseudo second order adsorption mechanism is predominant and that the rate of DBT adsorption process is controlled by more than one-step.

Conclusion

The present paper shows that the mesoporous carbon(MCG) could be synthesized by liquid infiltration of gelatin onto a SBA-48 silica template with carbonization, pyrolysis and silica removal step. The SAXRD, TEM and surface area analysis show that the MCG has the textural properties of mesoporous carbon with surface area, average pore size and volume pore and mesoporous quantity of 760 m^2/g; 5.2 nm and 0.999 cm^3/g and 74 %, respectively. The MCG was used as adsorbent for the removal of sulfuric compound (DBT) in the fuels. Equilibrium between the available of DBT in the solution and on the surface was practically achieved in 70 min. The kinetic adsorption processes was well described by irreversible pseudo second order model. Langmuir isotherm represented the equilibrium adsorption show the maximum adsorption capacity being 66,6 mg g^{-1}. The adsorption of DBT onto the MCG was found to be endothermic in nature with the heat of adsorption being 18.5 kJ/mol.

Acknowledgement

This work was financially supported by The Indonesian Ministry of Research, Technology, and Higher Education under research Grand of Penelitian Unggulan Perguruan Tinggi Universitas Gadjah Mada (Contract number: 907/UN1.P.III/LT/DIT-LIT/2016).

References

1. Maiyalagan, T., Nassr, A. B. a., Alaje, T. O., Bron, M.andScott, K. Three-dimensional cubic ordered mesoporous carbon (CMK-8) as highly efficient stable Pd electro-catalyst support for formic acid oxidation. Journal of Power Sources, 2012, 211, 147–153.

2. Haque, E., Khan, N. A.andTalapaneni, S.E., Vinu,A.,Jegal, J., Adsorption of Phenol on Mesoporous Carbon CMK-3: Effect of Textural Properties. Microporous and Mesoporous Materials, 2010, 31, 1638–1642.
3. Hou, Y., Guo, L.andWang, G., Synthesis and electrochemical performance of ordered mesoporous carbons with different pore characteristics for electrocatalytic oxidation of hydroquinone,Journal of Electroanalytical Chemistry, 2008, 617, 211–217.
4. Vinu, A., Anandan, S., Anand, C., Srinivasu, P., Ariga, K., Mori. T., Fabrication of partially graphitic three-dimensional nitrogen-doped mesoporous carbon using polyaniline nanocomposite through nanotemplating method.Microporous and Mesoporous Materials, 2008, 109, 398–404.
5. Pang, J., Ford, C.andTan, G. Mcpherson, G., John, G., Vijay T., Yungfeng, L.,Synthesis of mesoporous carbon using enzymatically polymerized polyphenolic precursor and simultaneously assembled silica template.Microporous and Mesoporous Materials, 2005, 85, 293–296.
6. Liu, Y. R. Microporous and Mesoporous Materials One-pot route to synthesize ordered mesoporous polymer/silica and carbon/silica nanocomposites using poly(dimethylsiloxane) – poly (ethylene oxide) (PDMS – PEO) as co-template. Microporous and Mesoporous Materials, 2009, 124, 190–196.
7. Kruk, M., Kohlhaas, K.M., Dufour, B.,Celer, E. B., Jaroniec, M., Partially graphitic, high-surface-area mesoporous carbons from polyacrylonitrile templated by ordered and disordered mesoporous silica.Microporous and Mesoporous Materials, 2007, 102, 178–187.
8. Shanmugam, M., Abilarasu, A., and Somanathan, T., Catalytic influence of Mo/SBA-15 towards the transesterification reaction using waste cooking oil palm oi., International Journal of ChemTech Research, 2014-2015, 7(2), 499-503.
9. Ge, J., Shi, J.andChen, L. Gelatin-based carbon microspheres with a foam-like core / solid shell structure. Carbon, 2008, 47, 1192–1195.
10. Hsu, C., Lin, H., Tang, C.andLin, C. Synthesis of mesoporous silica and mesoporous carbon using gelatin as organic template. Mesostructured Material, 2007, 385–388.
11. Ulfa, M., Trisunaryanti, W., Falah, I. I.andKartini, I., Synthesis of mesoporous carbon using gelatin as source of carbon by hard template technique and its characterizations. Journal of Applied Chemistry, 2014, 4, 1–7.
12. Ulfa, M., Trisunaryanti, W., Falah, I. I.andKartini, I. Nitrogen Sorption Evaluation of the Porous Carbon.Journal of Chemical Engineering and Chemistry Research, 2014, 1, 1–5.
13. Ulfa, M., Trisunaryanti, W., Falah, I. I.andKartini, I. Studies of kinetic on thermal decomposition of mesoporous carbon of gelatin by thermogravimetric technique. International Journal of Innovation and Applied Studies, 2014, 7, 849–856.
14. Salman, N., Jouhar, J., KaraBet, F., AL-Shnani, F., Deep desulfurization of hydrotreated diesel fraction using oxidation process followed by extraction. International Journal of ChemTech Research, 2015, 8(7), 96-103.
15. Gangwal, S. K.: Desulfurization for Fuel Cells. Fuel Cells: Technologies for Fuel Processing, Elsevier, 2011, 317–360.
16. Subha, E., Sasikala, S., Muthuraman, G., Removal of Phosphate from wastewater using natural adsorbents. International Journal of ChemTech Research, 2015, 7(7), 3095-3099.
17. Sangeetha, K., Vasugi, G., Girija, E.K., Removal of lead ions from aqueous solution by novel hydroxyapatite/alginate/gelatin composites. International Journal of ChemTech Research, 2015, 8(5), 117-125.
18. Ho, Y.S. Citation review of Lagergren kinetic rate equation on adsorption reactions. Akadémiai Kiadó, Budapest and Kluwer Academic Publisher., Dordrecht Scientometrics, 2004, 59, 171–177.
19. Bu, Jie.,Loh, G., Gwie, C G., Dewiyanti, S., Tasrif, M., Borgna, A., Desulfurization of diesel fuels by selective adsorption on activated carbons: Competitive adsorption of polycyclic aromatic sulfur heterocycles and polycyclic aromatic hydrocarbon.Chemical Engineering Journal, 2011, 166, 207–217.
20. Zhou, A., Ma, X.andSong, C. Applied Catalysis B : Environmental Effects of oxidative modification of carbon surface on the adsorption of sulfur compounds in diesel fuel. Applied Catalysis B: Environmental, 2009, 87, 190–199.
21. Ma, X., Velu, S., Kim, J. H.andSong, C. Deep desulfurization of gasoline by selective adsorption over solid adsorbents and impact of analytical methods on ppm-level sulfur quantification for fuel cell applications.Applied Catalysis B: Environmental, 2005, 56, 137–147.
22. Contreras, R. Bauerle, P., Schmelzer, M.andRoth, S., 2008. Transformation of thiophene, benzothiophene and dibenzothiophene over Pt/HMFI, Pt/HMOR and Pt/HFAU: Effect of reactant

molecular dimensions and zeolite pore diameter over catalyst activity.Catalysis Today, 2008, 130(2-4), 320–326.
23. Kluson, P. &Scaife, S.J., Pore Size Distribution Analysis of Structure Different Microporous Carbons–Theoretical Evaluation Based on Density Functional Theory and Nitrogen and Argon Experimental Adsorption Isotherms at 77 K. Microporous and Mesoporous Materials, 2001, 15(3), 117–125.
24. Ladavos, K., Katsoulidis, A.P., Iosifidis, A., Triantafyllidis, K.S., Pinnavaia, T.J., Pomonis, P.J. 2012. The BET equation, the inflection points of N_2 adsorption isotherms and the estimation of specific surface area of porous solids. Microporous and Mesoporous Materials, 2012, 151, 126–133.
25. Viswanath, S.G. & Gupta, M.C., 1997, The importance of the inflection point in nonisothermal analysis : New derivative methods. Microporous and Mesoporous Materials, 1997, 292, 151–157.
26. Zhu, Z. W., Yue, K.andHe, B.,HRTEM of negative replicas of mesoporous silica. Studies in Surface Science and Catalysis, 2004, 154, 924–930.
27. Steen, E. Van, Callanan, L. H., Oliveira, D., Federal, U.andCarlos, D. S. Phase Transformation Of Amorphous Sba-15 Pore Walls Into Microporous MFI Structure.Studies in Surface Science and Catalysis, 2005, 154, 541–549.
28. Diaz, I.andMayoral, A. TEM studies of zeolites and ordered mesoporous materials.Micron, 2011, 42, 512–527.
29. Lin, H., Chun-Yi, C.-C.andChih-Yuan, Tang, C.-Y. L. Synthesis of p6mm hexagonal mesoporous carbons and silicas using Pluronic F127 – PF resin polymer blends.Microporous and Mesoporous Materials, 2006, 93, 344–348.
30. Hodgkins, A. E., Sen, R. P.andAnderson, T. HRTEM Imaging Of Mesoporous Phase Transition From Hexagonal P6mm To Cubic La 3d Symmetry.Studies in Surface Science and Catalysis, 2005, 154, 400–407.
31. Hou, Y., Guo, L.andWang, G. Synthesis and electrochemical performance of ordered mesoporous carbons with different pore characteristics for electrocatalytic oxidation of hydroquinone. Journal of Electroanalytical Chemistry, 2008, 617, 211–217.
32. Karakassides, M.A., Synthesis and Characterization of Mesoporous Carbon Hybrids for Environmental Applications.Materials Chemistry and Physics, 2011, 17, 21–27.
33. Li, H. Sakamoto, Y., Li, Y., Terasaki, O., Synthesis of carbon replicas of SBA-1 and SBA-7 mesoporous silicas, 2006, 95, pp.193–199. Li, H.,
34. Salim I, Trisunaryanti W, Triyono, Arryanto Y. Hydrocracking of Coconut Oil into Gasoline Fraction using Ni/Modified Natural Zeolite Catalyst. International Journal of ChemTech Research., 2016, 9(4): 492-500.

*****